

## МОДИФИКАЦИЯ ПОВЕРХНОСТИ И РАСПЫЛЕНИЕ СПЛАВОВ FeCrAl ПРИ ВОЗДЕЙСТВИИ НИЗКОЭНЕРГЕТИЧЕСКОЙ ВОДОРОДНОЙ ПЛАЗМЫ

Г. Д. ТОЛСТОЛУЦКАЯ<sup>1)</sup>, М. А. ТИХОНОВСКИЙ<sup>1)</sup>,  
В. Н. ВОЕВОДИН<sup>1),2)</sup>, А. В. НИКИТИН<sup>1)</sup>, А. С. ТОРТИКА<sup>1)</sup>, Р. Л. ВАСИЛЕНКО<sup>1)</sup>

<sup>1)</sup>Институт физики твердого тела, материаловедения и технологий  
Национального научного центра «Харьковский физико-технический институт»,  
ул. Академическая, 1, 61108, г. Харьков, Украина

<sup>2)</sup>Харьковский национальный университет им. В. Н. Каразина,  
площадь Свободы, 4, 61022, г. Харьков, Украина

В работе исследованы процессы распыления и модификации поверхности коммерческих и экспериментальных сплавов FeCrAl, легированных иттрием, молибденом и цирконием. С помощью сканирующей электронной микроскопии показано, что под воздействием низкоэнергетической (500 эВ) водородной плазмы с потоком около  $3,2 \cdot 10^{20} \text{ м}^{-2} \cdot \text{с}^{-1}$  и флюенсом  $4 \cdot 10^{24} \text{ м}^{-2}$  при комнатной температуре морфология поверхности развивается вследствие образования канавок вдоль границ зерен, макро- и микротрещин, а также ямок, обусловленных распылением преципитатов. Определение состава последних энергодисперсионным рентгеновским спектрометром позволило

### Образец цитирования:

Толстолуцкая ГД, Тихоновский МА, Воеводин ВН, Никитин АВ, Тортика АС, Василенко РЛ. Модификация поверхности и распыление сплавов FeCrAl при воздействии низкоэнергетической водородной плазмы. *Журнал Белорусского государственного университета. Физика*. 2019;3: 73–80 (на англ.).  
<https://doi.org/10.33581/2520-2243-2019-3-73-80>

### For citation:

Tolstolutskaya GD, Tikhonovsky MA, Voyevodin VN, Nikitin AV, Tortika AS, Vasilenko RL. Surface modification and sputtering of FeCrAl alloys exposed to low-energy hydrogen plasmas. *Journal of the Belarusian State University. Physics*. 2019;3:73–80.  
<https://doi.org/10.33581/2520-2243-2019-3-73-80>

### Авторы:

**Галина Дмитриевна Толстолуцкая** – доктор физико-математических наук, профессор, начальник лаборатории физики взаимодействия ионных пучков с материалами.

**Михаил Андреевич Тихоновский** – кандидат физико-математических наук; начальник лаборатории наноматериалов.

**Виктор Николаевич Воеводин** – член-корреспондент НАН Украины, доктор физико-математических наук, профессор, директор<sup>1)</sup>, профессор кафедры реакторного материаловедения и физических технологий физико-технического факультета<sup>2)</sup>.

**Аркадий Валерьевич Никитин** – кандидат физико-математических наук; научный сотрудник лаборатории физики взаимодействия ионных пучков с материалами.

**Александр Степанович Тортика** – начальник группы лаборатории наноматериалов.

**Руслан Леонидович Василенко** – младший научный сотрудник лаборатории электронно-микроскопических исследований структуры облученных материалов.

### Authors:

**Galina D. Tolstolutskaya**, doctor of science (physics and mathematics), full professor; head of the laboratory of physics of interaction of ion beams with materials.

[g.d.t@kipt.kharkov.ua](mailto:g.d.t@kipt.kharkov.ua)

<https://orcid.org/0000-0003-3091-4033>

**Michael A. Tikhonovsky**, PhD (physics and mathematics); head of the laboratory of nanomaterials.

[tikhonovsky@kipt.kharkov.ua](mailto:tikhonovsky@kipt.kharkov.ua)

<https://orcid.org/0000-0001-5889-0366>

**Victor N. Voyevodin**, corresponding member of the National Academy of Sciences of Ukraine, doctor of science (physics and mathematics), full professor; director<sup>a</sup> and professor at the department of structural reactor materials and physical technology, faculty of physics and technology<sup>b</sup>.

[voyev@kipt.kharkov.ua](mailto:voyev@kipt.kharkov.ua)

<https://orcid.org/0000-0003-2290-5313>

**Arkadiy V. Nikitin**, PhD (physics and mathematics); researcher at the laboratory of physics of interaction of ion beams with materials.

[gtolst@ukr.net](mailto:gtolst@ukr.net)

<https://orcid.org/0000-0001-8853-1145>

**Aleksander S. Tortika**, head of the group at the laboratory of nanomaterials.

[tortika@kipt.kharkov.ua](mailto:tortika@kipt.kharkov.ua)

<https://orcid.org/0000-0002-0813-341X>

**Ruslan L. Vasilenko**, junior researcher at the laboratory of electron-microscopic investigations of the structure of irradiated materials.

[rvasilenko@kipt.kharkov.ua](mailto:rvasilenko@kipt.kharkov.ua)

<https://orcid.org/0000-0002-4029-9727>

установить, что оксид алюминия преимущественно распределен в зернах сплавов на основе FeCrAl, а оксиды иттрия локализованы по границам зерен. Результаты эрозионных исследований показали, что коэффициенты распыления для водорода у всех сплавов составляют 1,05–0,38 ат./ион и не превышают таковых для чистого железа и хрома в опубликованных данных. Для экспериментальных сплавов, легированных иттрием и молибденом, получено, что коэффициенты распыления в несколько раз меньше, чем у стали SS304, и только в полтора раза выше по сравнению с вольфрамом.

**Ключевые слова:** ферритные сплавы FeCrAl; водородная плазма; морфология поверхности; эрозия; коэффициент распыления.

**Благодарность.** Работа выполнена при финансовой поддержке Национальной академии наук Украины (программа «Поддержка развития приоритетных направлений научных исследований») (КПКВК 6541230)).

## SURFACE MODIFICATION AND SPUTTERING OF FeCrAl ALLOYS EXPOSED TO LOW-ENERGY HYDROGEN PLASMAS

G. D. TOLSTOLUTSKAYA<sup>a</sup>, M. A. TIKHONOVSKY<sup>a</sup>,  
V. N. VOYEVODIN<sup>a, b</sup>, A. V. NIKITIN<sup>a</sup>, A. S. TORTIKA<sup>a</sup>, R. L. VASILENKO<sup>a</sup>

<sup>a</sup>*Institute of Solid State Physics, Material Science and Technology,  
National Science Center «Kharkov Institute of Physics and Technology»,  
1 Akademicheskaya Street, Kharkiv 61108, Ukraine*

<sup>b</sup>*V. N. Karazin Kharkiv National University, 4 Svobody Square, Kharkiv 61022, Ukraine*

*Corresponding author: G. D. Tolstolutskaia (g.d.t@kipt.kharkov.ua)*

In the present paper processes of sputtering and surface modification of commercial and experimental FeCrAl composites alloyed with yttrium, molybdenum and zirconium were investigated. Using a field-emission scanning electron microscope, it was shown that under the influence of low-energy (500 eV) hydrogen plasma with a flux about  $3.2 \cdot 10^{20} \text{ m}^{-2} \cdot \text{s}^{-1}$  and fluence  $4 \cdot 10^{24} \text{ m}^{-2}$  at  $T_{\text{room}}$ , surface morphology develops due to the formation of grooves along grain boundaries, macro- and microcracks, as well as intragranular pits due to the sputtering of precipitates. Determination of the composition of precipitates by an energy dispersive X-ray spectrometer allowed to establish that aluminum oxide is preferentially distributed in the grains of FeCrAl-based alloys, and yttrium oxides are localized along grain boundaries. Results of erosion studies indicated that the sputtering yields for hydrogen on all alloys are 1.05–0.38 at./ion and doesn't exceed those for published data for pure iron and chromium. For experimental alloys doped with yttrium and molybdenum found that the obtained sputtering coefficients were in several times lower than for steel SS304 and only one and a half times higher compared to tungsten.

**Keywords:** FeCrAl ferritic alloys; hydrogen plasma; surface morphology; erosion; sputtering yield.

**Acknowledgements.** The work was financially supported by the National Academy of Sciences of Ukraine (program «Support of the development of main lines of scientific investigations») (КПКВК 6541230)).

### Introduction

A recent interest in Accident Tolerant Fuel cladding for light water reactors has restored the attention to the iron-chromium-aluminum (FeCrAl) ferritic alloy system, which have been used in the non-nuclear industry for over eight decades [1]. FeCrAl alloys have been also considered as a promising candidate for a fusion blanket application [2].

To assess the possibility to use the FeCrAl alloys as plasma-facing materials, there is a need to examine a behavior of these materials under plasma exposure. Due to the large power flux and steady-state environment expected in DEMO the areas of plasma-facing materials will be subjected to largest charge-exchange neutral fluxes at very low energies of the order of 1000 eV and below. Sputtering of plasma-facing materials due to interaction with energetic ions (particularly hydrogen isotopes) is an essential issue in magnetically confined fusion devices because it is directly related to impurity generation as well as to the lifetime of plasma-facing components [3; 4]. For a better understanding of the sputtering processes on FeCrAl alloys it is necessary firstly to know the sputtering of each alloyed element as a reference. However, sputtering data for these elements are still quite limited and for FeCrAl as whole also.

The goal of this work is to experimentally determine the sputtering yields and surface modification of FeCrAl alloys exposed to low-energy, high-flux hydrogen plasma and compares the obtained data of sputtering yields with existing published data for Fe, Cr, SS304 and W.

### Material and methods

Five samples (# 1–5) were selected as materials for the study; two of them (# 1 и 2) were commercial Kanthal-type alloys H23U5T. Sample # 1 (round bar 20 mm in diameter) was in delivery state, sample # 2 was the same rod, remelted by the argon-arc method and casted into a cylindrical copper mold 10 mm in diameter. Experimental alloys # 3–5 were melted at the same conditions. High purity metals were used as the raw materials (armco iron, aluminum 99.99 %, electrolytic chromium 99.99 %, molybdenum 99.9 % and zirconium 99.9 %). At least five melting with turning over at each remelting were performed to improve the chemical homogeneity of the ingots. The final solidified ingots were cylindrical bars with a diameter of 10 mm and height of 30 mm, weighing  $\approx 30$  g.

Microstructure analysis and chemical analysis at individual «points» (size of 5–10  $\mu\text{m}^2$ ) showed that aluminum, chromium, silicon, manganese, nickel and molybdenum were fairly uniform distributed in the main matrix phase. In other words, these elements form substitution solid solutions with iron, which is consistent with the known phase diagrams of iron-based binary systems [5]. At the same time, titanium in commercial alloy (samples # 1 and 2) is distributed very unevenly. The matrix phase contains 2–3 times less titanium (0.06–0.13 %) than all over the sample.

The disk-shaped specimens, 10 mm in diameter and about 0.8 mm in thickness, were cut from bar of each material. The surface of each disk was polished mechanically to a mirror-like and then electropolished in a standard electrolyte to remove any mechanically damaged near-surface layer. Prepared specimens have been irradiated with hydrogen ions using glow gas-discharge plasma electrodes at 1000 V. The central portion of the specimen was irradiated through an aperture, providing an easily-observed boundary between irradiated and unirradiated regions. The design and principle of operation of the gaseous plasma source used for irradiation of the samples is described in detail in [6].

The dominant ion component generated in the ion source is  $\text{H}_2^+$ . This ion was chosen as the bombarding species to achieve higher particle fluxes. These molecular  $\text{H}_2^+$  ions are considered to be identical to 2 individual H ions impinging with the same velocity as the molecular ion. Breakup of the molecular  $\text{H}_2^+$  ions on the target surface results in emergence of two H atoms with the kinetic energy of 1/2 experimentally applied ion energy and the flux is two times the measured ion flux. In our experiments the FeCrAl targets were sputtered with atomic  $\text{H}^+$  ions at the ion energy of 500 eV with flux of  $3.2 \cdot 10^{20} \text{ m}^{-2} \cdot \text{s}^{-1}$ . The maximum irradiation fluence was  $4 \cdot 10^{24} \text{ m}^{-2}$ . The experimental ion flux and fluence were calculated from the measured ion currents and beam spot areas.

The specimen temperature was continuously monitored using a thermocouple in the base of the specimen holder and was attached to the lower surface of specimen. Temperature maintenance on the samples in this device was achieved either by resistive heating or liquid nitrogen cooling and found to be around  $T_{\text{room}}$ . The temperature was maintained within  $\pm 2.5$  K.

The erosion yield was primarily evaluated by a weight-loss technique. Before and after plasma exposure, the weight of each target was measured by a microbalance system, and the erosion rate was then calculated from the weight loss and the total hydrogen fluence. Typical weight losses were between 20 and 160  $\mu\text{g}$ ; the uncertainty in the weight loss determination is estimated to be  $\pm 2$   $\mu\text{g}$ .

The surface morphology of the targets exposed to the hydrogen plasma was examined with a field-emission scanning electron microscope JEOL JSM-6710F equipped with an energy dispersive X-ray (EDX) spectrometer.

### Results and discussion

**Surface morphology and chemical compositions.** SEM examination of targets exposed to the hydrogen plasmas has revealed that surface modification of FeCrAl alloys resulted from the variations of sputtering erosion of different topographical structures.

The surface microstructure of the commercial alloy in the initial state is typical for recrystallized material with a grain size  $\geq 100$   $\mu\text{m}$  and with a lot of precipitates (fig. 1, a). Figure 1, b, shows that after irradiated with hydrogen gas-discharge plasmas the surface of samples # 1 have the almost rectangular cracks covering over the entire specimen irradiated surface. It should be noted that the development of cracks does not always coincide with the boundaries of the grains. This process can occur mainly at the sites of localization of impurities or stresses.

The ingot from commercial alloy (samples # 2) has microstructure with a larger grain size ( $\sim 100$   $\mu\text{m}$  up to 1 mm) (fig. 1, c). After sputtering the grain boundaries in this case are destroyed more strongly in comparison with

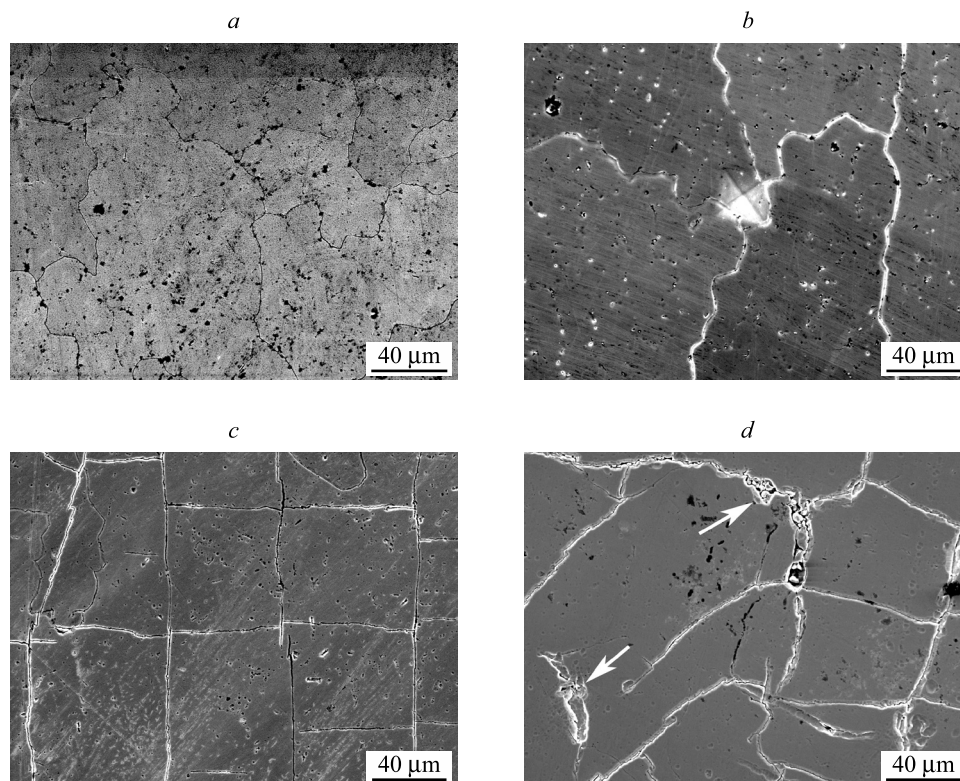


Fig. 1. SEM images of the initial samples surface # 1 (a) and # 2 (b), details of the surface after sputtering of commercial (c) and remelted samples (d). The trace from the indenter is also visible in the image (b)

the sample in the initial state. The surface morphology is developed due to generation of grooves along grain boundaries, macro and micro cracks and intragranular pits due to the sputtering of precipitates. The chemical compositions for each alloy are specified in the table 1. It should be noted that elements concentration given in the table as «unirradiated» and «sputtered» was determined by scanning over a sufficiently large area (about  $1 \text{ mm}^2$ ) and as «precipitate» at individual «points» (size of  $5\text{--}10 \text{ }\mu\text{m}^2$ ).

Heavily etched sections of grain boundaries (indicated by arrows in fig. 1, d) of remelted FeCrAl (samples # 2) contains 2–3 times more titanium ( $\sim 0.6 \text{ wt. } \%$ ) and silicon ( $\sim 2.4 \text{ wt. } \%$ ) than all over the sample. The concentration Fe, Cr and Al practically does not change during the process of sputtering compared to the initial composition.

Table 1

Typical nominal and measured compositions and after sputtering of as-received and remelted FeCrAl alloys exposed to hydrogen plasma

Sample	Concentration, wt. %						
	Fe	Cr	Al	Other elements			
				Si	Ti	Mn	Ni
# 1. Initial bar (commercial): nominal measured (unirradiated) sputtered	Bal.	22–24	5.0–5.8	To 0.5	0.2–0.5	To 0.3	To 0.6
	Bal.	$22.65 \pm 0.05$	$4.04 \pm 0.02$	$0.53 \pm 0.03$	$0.21 \pm 0.08$	$0.28 \pm 0.06$	$0.13 \pm 0.06$
	Bal.	$22.62 \pm 0.02$	$4.19 \pm 0.04$	$0.23 \pm 0.06$	$0.55 \pm 0.07$	–	–
# 2. Remelted: nominal measured (unirradiated) sputtered precipitate	Bal.	22–24	5.0–5.8	To 0.5	0.2–0.5	To 0.3	To 0.6
	Bal.	$22.52 \pm 0.07$	$4.06 \pm 0.05$	$0.58 \pm 0.03$	$0.22 \pm 0.08$	$0.29 \pm 0.06$	$0.14 \pm 0.06$
	Bal.	$22.15 \pm 0.03$	$4.04 \pm 0.04$	$0.62 \pm 0.06$	–	–	–
	Bal.	$22.51 \pm 0.05$	$4.26 \pm 0.03$	$2.42 \pm 0.07$	$0.60 \pm 0.07$	–	–

Samples (ingots) # 3–5 have anisotropic coarse-grained microstructure (grain size near several millimeters), wherein some grains are elongated in the direction of heat sink. The chemical composition for alloy # 3–5 is given in table 2. The yttrium distribution in the ingots is of greatest interest. Microanalysis showed that

there is no yttrium in the grains body of the matrix phase (its concentration is less than detection limit of about 0.1 at. %). The main amount of yttrium is concentrated at grain boundaries or in precipitations. These precipitations are yttrium oxides. Such yttrium distribution is associated with its low solubility in iron and, as a consequence, in the matrix phase [5].

Table 2

Nominal and measured compositions of FeCrAl alloys # 3–5

Sample	Concentration, wt. %					
	Fe	Cr	Al	Other elements		
				Y	Mo	Zr
# 3 (ingot): nominal measured	Bal.	21.0	6.0	1.0	–	–
	Bal.	21.84 ± 0.1	6.07 ± 0.05	0.83	–	–
# 4 (ingot): nominal measured	Bal.	21.0	6.0	1.0	2.0	–
	Bal.	21.82 ± 0.05	5.35 ± 0.05	0.53 ± 0.03	2.58 ± 0.05	–
# 5 (ingot): nominal measured	Bal.	23.0	9.0	1.0	2.0	2.0
	Bal.	23.86 ± 0.19	8.55 ± 0.13	0.66 ± 0.02	2.07 ± 0.01	1.87 ± 0.16

SEM examination of the FeCrAl alloys targets (# 3 and 4) exposed to the 500 eV hydrogen plasmas has revealed that only already described well-known topographical structures are observed on the surfaces (fig. 2, *a – c*). Spectra 1 and 2 were taken on the surface of FeCrAl after sputtering, where spectrum 1 was taken in the middle of the grain and spectrum 2 from precipitate at the grain boundary (table in fig. 2). Comparison of the compositions from these spectra had shown that the aluminum oxide preferential located in grain and yttrium oxide at the grain boundary. Molybdenum is practically uniformly distributed in the main matrix phase on a sputtered surface.

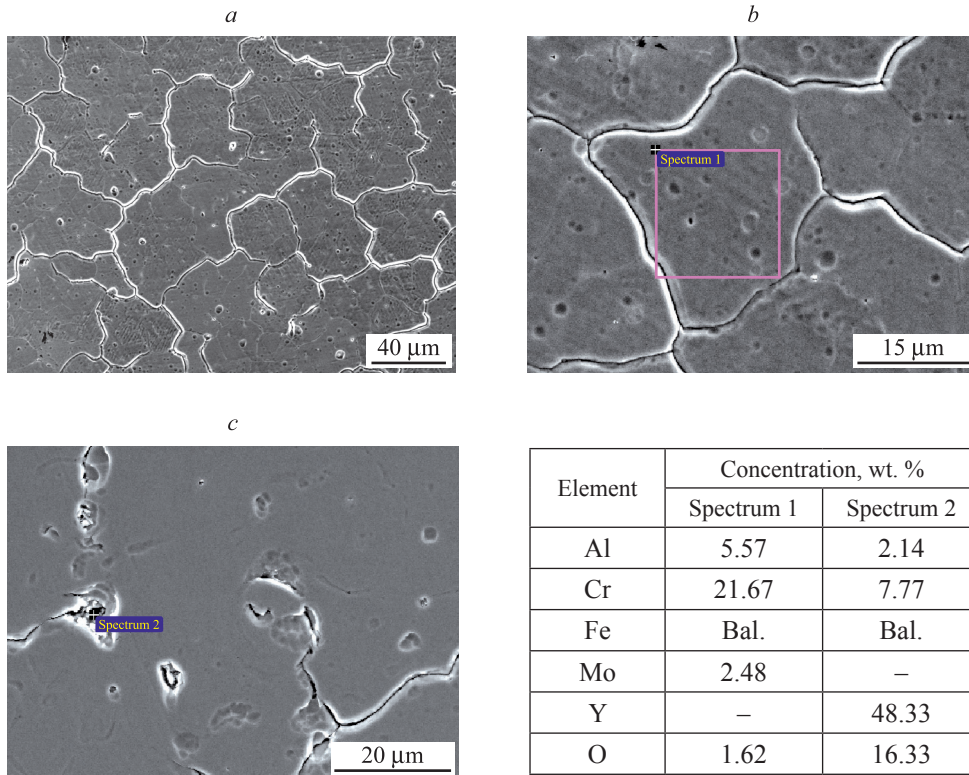


Fig. 2. SEM images of the surface of FeCrAl doped with yttrium + molybdenum after sputtering (*a*), detail of the surface with cracks along grain boundaries (*b*) and precipitates (*c*) and the EDS analyses from the points marked in the images (*b*, *c*)

A significant change in the microstructure FeCrAl is observed when besides alloying with yttrium and molybdenum it was also added zirconium (sample # 5). Firstly, grain refinement occurs, and secondly, the eutectic component appears at the grain boundaries in initial FeCrAl alloys doped with yttrium + molybdenum + zirconium (fig. 3, *a, b*). As in the case of yttrium, the concentration of zirconium in the matrix phase is below the detection limit due to its low solubility in iron [5] (see spectrum 1 in the table in fig. 3). The zirconium concentration in the eutectic is  $15.2 \pm 1.2 \%$  (average value over several measurements), which is close to eutectic concentration in binary system Fe–Zr [7]. Average values of other elements concentration in eutectic are given in the table in fig. 3 (spectrum 2). Thus, almost all zirconium and yttrium are concentrated in the eutectic; chromium is near uniformly distributed between matrix phase and eutectic, although its concentration in eutectic is lower than in matrix phase.

The surface morphology that is developed due to the hydrogen plasma exposure of FeCrAl alloys doped with yttrium + molybdenum + zirconium is shown in fig. 3, *c*. As well as for other modifications of the alloys it can be seen the grooves along the grain boundaries and cracks develop as a result of sputtering. The cracks have both radial orientation and form a «cellular» structure. Location of grooves and cracks on the surface of the samples repeats the distribution of doping impurities of yttrium, molybdenum and zirconium (see fig. 3, *a*). Spectrum 3 (see table in fig. 3) shows the composition of precipitates appearing at the grain boundaries after sputtering represented mainly by zirconium oxides.

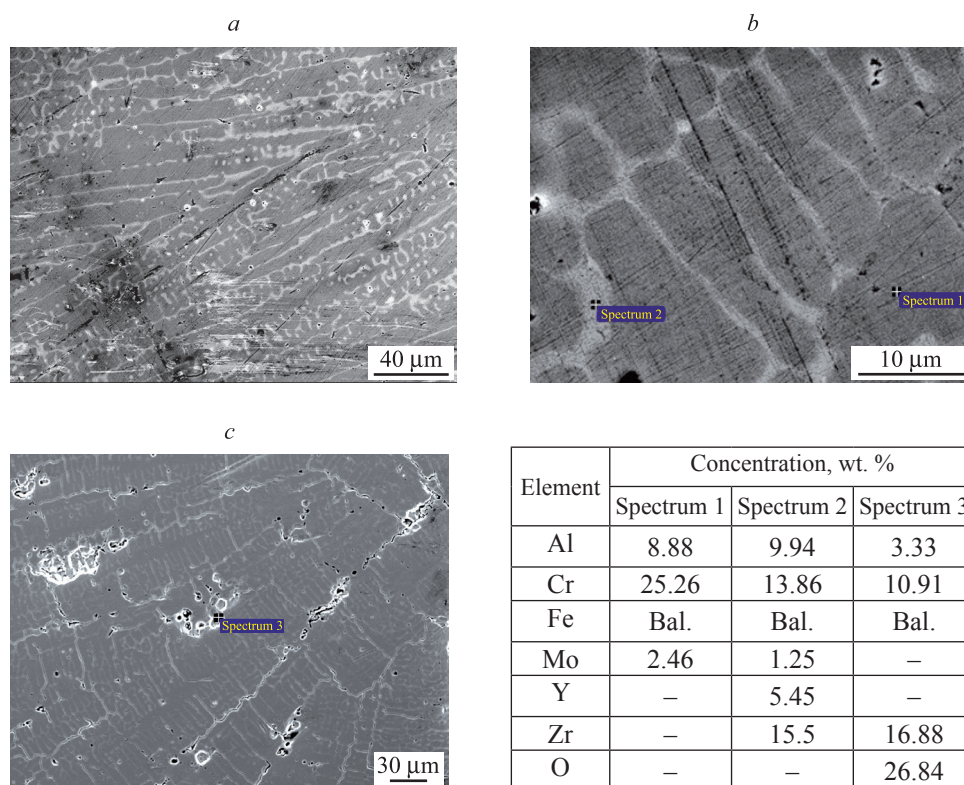


Fig. 3. SEM images of the initial surface of FeCrAl doped with molybdenum + yttrium + zirconium (*a, b*), detail of the surface after sputtering (*c*) and the EDS analyses from the points marked in the images (*b, c*)

**Sputtering erosion.** As noted above in our experiment's hydrogen plasmas sputtering erosion of FeCrAl alloys was obtained using the weight loss technique. The sputtering yield was then calculated from the weight loss and the total hydrogen fluence.

It should be noted that the following considerations were taken into account when the process of sputtering of FeCrAl was studied. Impurity ions with heavier mass than the main component ions might increase the sputtering rate. They could specially have large effects on the data from light-ion plasmas, i. e., hydrogen and deuterium plasma. Spectroscopic measurement showed that the impurity concentration was less than 0.1 % [6].

The phenomenon of self-sputtering might also introduce systematic error into the results. The mechanism of self-sputtering is as follows; sputtered atoms are ionized in the plasma, flow back to the sample, and hit it after acceleration in the sheath. Therefore, it is necessary to check how large a fraction of sputtered atoms flow back to the sample. The concentration of sputtered atoms in the plasma was measured as a function of the

distance from the sample by the use of the spectroscopic method, and it was concluded that the backflow was not large enough to affect the sputtering yield measurements [8].

Figure 4 shows the results for the sputtering yield of FeCrAl alloys in comparison with published data of pure iron, chromium, SS304 and W sputtering yields determined experimentally and by numerical simulation [9; 10].

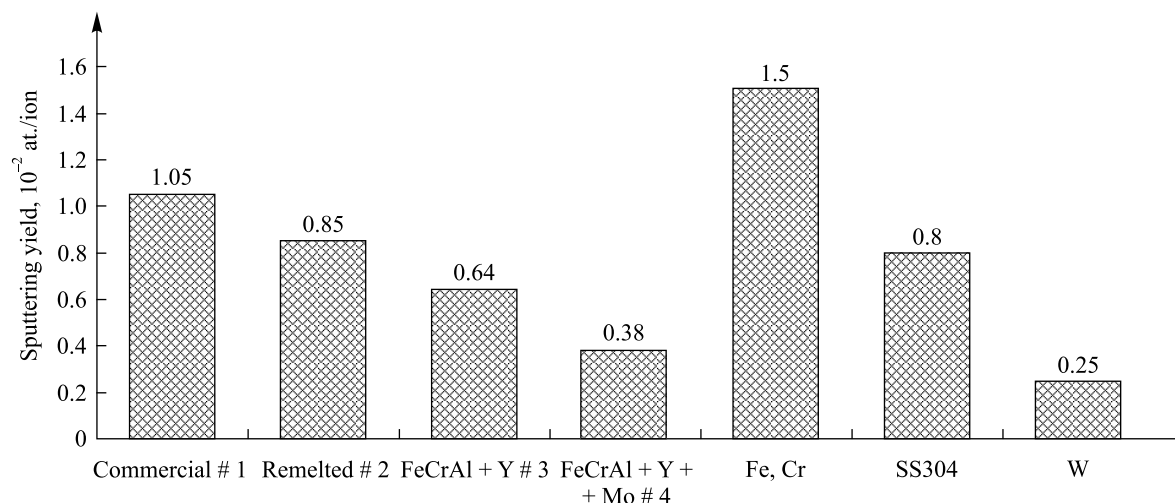


Fig. 4. Experimentally determined sputtering yields of FeCrAl alloys. For comparison sputtering yields of Fe, Cr, SS304 and W are shown

As seen in fig. 4, values of the experimentally measured sputtering yield of the FeCrAl alloys doped with yttrium exposed to the H plasma are 30–50 % lower in comparison with commercial and remelted samples. Additional alloying with yttrium and molybdenum leads to a decrease in the sputtering coefficient to  $0.38 \cdot 10^{-2}$  at./ion those almost three times as less in comparison with published data for pure iron, chromium and SS304 steel. It should be noted that the sputtering coefficients of the alloy with the addition of yttrium and molybdenum are only one and a half times higher compared to tungsten. At present, the sputtering coefficient of tungsten with hydrogen isotopes is considered to be the lowest. However, W-sputtering and an unfavorable neoclassical transport of W-impurities may lead to W accumulation which requires adequate avoidance techniques of large central radiation losses [11]. FeCrAl alloys with middle-Z admixed elements doped yttrium and molybdenum can be considered as a candidate for armor materials of plasma-facing components of tokamak devices.

### Conclusion

The sputtering yields and surface modification of commercial Kanthal-type alloys H23U5T and his remelted version, and experimental alloys doped with yttrium + molybdenum + zirconium exposed to low-energy (500 eV), high-flux ( $\sim 3.2 \cdot 10^{20} \text{ m}^{-2} \cdot \text{s}^{-1}$ ) with fluence  $4 \cdot 10^{24} \text{ m}^{-2}$  of hydrogen plasma are studied. On the FeCrAl alloys surfaces exposed to the H plasmas at room temperature the grooves along grain boundaries, macro and micro cracks and intragranular pits due to the sputtering of precipitates are developed. In the initial state of components of alloys aluminum, chromium, silicon, manganese, nickel and molybdenum were fairly uniformly distributed in the main matrix phase and form substitutional solid solutions with iron. Titanium in commercial alloy is distributed very unevenly: the matrix phase contains 2–3 times less titanium (0.06–0.13 %) than all over the sample. The main amount of yttrium, as yttrium oxides, is concentrated at grain boundaries or in precipitations. The concentration of zirconium in the matrix phase is below the detection limit 0.1 at. %. However, the Zr component with concentration close to eutectic of binary system Fe–Fe<sub>2</sub>Zr appears at the grain boundaries. After exposure to hydrogen plasma it has been found that the aluminum oxides preferentially locate in grain but yttrium and zirconium oxides at the grain boundary. Molybdenum is practically uniformly distributed in the main matrix phase on a sputtered surface. The sputtering yields of commercial kanthal-type alloys H23U5T and his remelted version, and experimental FeCrAl alloys doped with yttrium + molybdenum + zirconium exposed to low-energy hydrogen plasma are 1.05–0.38 atoms per incident particle and not exceeding those for pure iron and chromium. For some compositions, e. g., FeCrAl alloys doped with yttrium + molybdenum, it is obtained sputtering coefficients in several times smaller than steel SS304 and only one and a half times higher compared to tungsten. Results reported in this work is thought to be of interest for an understanding of mechanisms of possible formation of erosion structures on the FeCrAl alloys surfaces under exposure to the hydrogen isotope plasmas and predicting possibilities of using these alloys as structural materials of fusion reactors.

## Библиографические ссылки

1. Yamamoto Y, Pint BA, Terrani KA, Field KG, Yang Y, Snead LL. Development and property evaluation of nuclear grade wrought FeCrAl fuel cladding for light water reactors. *Journal of Nuclear Materials*. 2015;467(2):703–716. DOI: 10.1016/j.jnucmat.2015.10.019.
2. Pint BA, Dryepont SN, Unocic KA, Hoelzer DT. Development of ODS FeCrAl for compatibility in fusion and fission energy applications. *Journal of the Minerals Metals & Materials Society*. 2014;66(12):2458–2466. DOI: 10.1007/s11837-014-1200-z.
3. Sigmund P. Theory of sputtering. I. Sputtering yields of amorphous and polycrystalline targets. *Physical Review*. 1969;184(2):383–345. DOI: 10.1103/PhysRev.187.768.
4. Roth J, Sugiyama K, Alimov V, Hoeschen T, Baldwin MJ, Doerner R. EUROFER as wall material: Reduced sputtering yields due to W surface enrichment. *Journal of Nuclear Materials*. 2014;454(1–3):1–6. DOI: 10.1016/j.jnucmat.2014.07.042.
5. Банных ОА, Будберг ПБ, Алисова СП. *Диаграммы состояния двойных и многокомпонентных систем на основе железа*. Москва: Металлургия; 1986. 440 с.
6. Nikitin AV, Tolstolutsкая GD, Ruzhytskyi VV, Voyevodin VN, Kopanets IE, Karpov SA, et al. Blister formation on 13Cr2MoNbVB ferritic-martensitic steel exposed to hydrogen plasma. *Journal of Nuclear Materials*. 2016;478:26–31. DOI: 10.1016/j.jnucmat.2016.05.032.
7. Резниченко ВВ, Сомов АИ, Тихоновский МА. Микроструктура и прочность эвтектической композиции Fe–Fe<sub>2</sub>Zr. *Физика металлов и металловедение*. 1973;37(3):657–659.
8. Bohdansky J. A universal relation for the sputtering yield of monatomic solids at normal ion incidence. *Nuclear Instruments and Methods in Physics Research Section B: Beam Interactions with Materials and Atoms*. 1984;2(1–3):587–591. DOI: 10.1016/0168-583X(84)90271-4.
9. Andersen HH, Bay HL. Sputtering yield measurements. In: Behrisch R, editor. *Sputtering by Particle Bombardment. I. Physical Sputtering of Single-Element Solids*. Berlin: Springer; 1981. p. 145–218.
10. Sugiyama K, Schmid K, Jacob W. Sputtering of iron, chromium and tungsten by energetic deuterium ion bombardment. *Nuclear Materials and Energy*. 2016;8:1–7. DOI: 10.1016/j.nme.2016.05.016.
11. Wiesen S, Groth M, Wischmeier M, Brezinsek S, Jarvinen A, Reimold F, et al. Plasma edge and plasma-wall interaction modelling: Lessons learned from metallic devices. *Nuclear Materials and Energy*. 2017;12:3–17. DOI: 10.1016/j.nme.2017.03.033.

## References

1. Yamamoto Y, Pint BA, Terrani KA, Field KG, Yang Y, Snead LL. Development and property evaluation of nuclear grade wrought FeCrAl fuel cladding for light water reactors. *Journal of Nuclear Materials*. 2015;467(2):703–716. DOI: 10.1016/j.jnucmat.2015.10.019.
2. Pint BA, Dryepont SN, Unocic KA, Hoelzer DT. Development of ODS FeCrAl for compatibility in fusion and fission energy applications. *Journal of the Minerals Metals & Materials Society*. 2014;66(12):2458–2466. DOI: 10.1007/s11837-014-1200-z.
3. Sigmund P. Theory of sputtering. I. Sputtering yields of amorphous and polycrystalline targets. *Physical Review*. 1969;184(2):383–345. DOI: 10.1103/PhysRev.187.768.
4. Roth J, Sugiyama K, Alimov V, Hoeschen T, Baldwin MJ, Doerner R. EUROFER as wall material: Reduced sputtering yields due to W surface enrichment. *Journal of Nuclear Materials*. 2014;454(1–3):1–6. DOI: 10.1016/j.jnucmat.2014.07.042.
5. Bannikh OA, Budberg PB, Alisova SP. *Diagrammy sostoyaniya dvoynnykh i mnogokomponentnykh sistem na osnove zheleza* [State diagrams of binary and multicomponent systems on the base of iron]. Moscow: Metallurgiya; 1986. 440 p. Russian.
6. Nikitin AV, Tolstolutsкая GD, Ruzhytskyi VV, Voyevodin VN, Kopanets IE, Karpov SA, et al. Blister formation on 13Cr2MoNbVB ferritic-martensitic steel exposed to hydrogen plasma. *Journal of Nuclear Materials*. 2016;478:26–31. DOI: 10.1016/j.jnucmat.2016.05.032.
7. Reznichenko VV, Somov AI, Tikhonovsky MA. [Microstructure and strength of the eutectic composition Fe–Fe<sub>2</sub>Zr]. *Fizika metallov i metallovedenie*. 1973;37(3):657–659. Russian.
8. Bohdansky J. A universal relation for the sputtering yield of monatomic solids at normal ion incidence. *Nuclear Instruments and Methods in Physics Research Section B: Beam Interactions with Materials and Atoms*. 1984;2(1–3):587–591. DOI: 10.1016/0168-583X(84)90271-4.
9. Andersen HH, Bay HL. Sputtering yield measurements. In: Behrisch R, editor. *Sputtering by Particle Bombardment. I. Physical Sputtering of Single-Element Solids*. Berlin: Springer; 1981. p. 145–218.
10. Sugiyama K, Schmid K, Jacob W. Sputtering of iron, chromium and tungsten by energetic deuterium ion bombardment. *Nuclear Materials and Energy*. 2016;8:1–7. DOI: 10.1016/j.nme.2016.05.016.
11. Wiesen S, Groth M, Wischmeier M, Brezinsek S, Jarvinen A, Reimold F, et al. Plasma edge and plasma-wall interaction modelling: Lessons learned from metallic devices. *Nuclear Materials and Energy*. 2017;12:3–17. DOI: 10.1016/j.nme.2017.03.033.

Received by editorial board 20.08.2019.